European Journal of Medicinal Chemistry 69 (2013) 711–718

Contents lists available at ScienceDirect

European Journal of Medicinal Chemistry

journal homepage: http://www.elsevier.com/locate/ejmech

Original article

Design and application of a rigid quinazolone scaffold based on two-face Bim α-helix mimicking

Zhichao Zhang [a, *], Xiaomeng Liang [a, b], Xiangqian Li [a], Ting Song [a], Qingbin Chen [c], Hongkun Sheng [a]

[a] State Key Laboratory of Fine Chemicals, School of Chemistry, Dalian University of Technology, Dalian 116012, People's Republic of China
[b] State Key Laboratory of Natural and Biomimetic Drugs, Peking University, Beijing 100191, People's Republic of China
[c] School of Life Science and Technology, Dalian University of Technology, Dalian 116024, People's Republic of China

ARTICLE INFO

Article history:
Received 7 May 2013
Received in revised form
9 September 2013
Accepted 11 September 2013
Available online 21 September 2013

Keywords:
α-Helix
Quinazolone
Two-faced
Mcl-1
Bcl-2

ABSTRACT

Based on our previous discovery of an anthraquinone scaffold mimicking two faces of Bim α-helix, we derived a quinazolone scaffold through structure simplification and optimization. It was inferred that a rigid bicyclic ring was necessary and efficient to maintain the two-faced binding mode. A novel dual inhibitor **6c** [6,7,8-trihydroxy-3-(2-hydroxy-5-methylbenzyl)-2-phenylquinazolin-4(3H)-one] was obtained based on this scaffold. **6c** exhibited dual binding activity with K_i values of 0.123 μM for Mcl-1 and 0.179 μM for Bcl-2.

© 2013 Elsevier Masson SAS. All rights reserved.

1. Introduction

Apoptosis is a critical process in both development and homeostasis of multicellular organisms [1,2]. Bcl-2 is the founding member of a protein family composed of pro- and anti-apoptotic molecules that serve as an essential control point in apoptosis, governing susceptibility to cell death [3].

Bcl-2 family members consist of anti-apoptotic members, such as Bcl-2 and Mcl-1. Pro-apoptotic members can be subdivided into multi-domain family members (Bax, Bak), containing multiple BH domains (BH1–BH4), and BH3-only proteins that contain only BH3 domain [1]. The BH3 domains of these pro-apoptotic molecules form an α-helical fold when bound to a groove lined by the BH1, BH2, and BH3 domains of anti-apoptotic proteins such as Bcl-2, a step thought to be important for apoptosis induction [4]. Therefore, strategies that target the functional BH3 binding groove of these pro-apoptotic members may provide a feasible mechanism for killing tumor cells [5].

Bim is a nonselective BH3-only protein, so the designed Bim BH3-mimetics could interact with anti-apoptotic Bcl-2 family proteins, and thus enable the apoptotic cascade leading to cell death [6,7].

A significant fraction of protein–protein interactions (PPIs) will require mimetics that array protein-like functionality on multiply faces [8]. The hotspots of Bim in complex with Mcl-1 and Bcl-2 are located on two faces of the Bim BH3 α-helix [7]. However the potent and dual inhibitors of Bcl-2 and Bcl-x_L, ABT-737 and nonpeptide α-helix mimicry terphenyl scaffolds can impart functionality from only one face of Bim and cannot mimic D67 which is on the opposite side of the α-helix and conserved in all BH3 domains [9,10].

Previously, we have reported a rigid-plan anthraquinone scaffold to mimic the structural binding features on two faces of the Bim BH3 α-helix [7]. Its derivatives exhibit nanomolar affinities toward the two proteins and specific antitumor abilities in cells. On basis of it, we derived a quinazolone scaffold through structural simplification and optimization process. Compound **6c** was obtained as a dual inhibitor of Bcl-2 and Mcl-1 proteins, with K_i values of 179 nM and 123 nM, respectively, and maintained the two-faced binding mode.

2. Chemistry

Compound **5** was prepared according to the method of Liu et al. [11]. Methyl ethers were deprotected sequentially using

* Corresponding author. Tel./fax: +86 411 84986032.
E-mail address: zczhang@dlut.edu.cn (Z. Zhang).

0223-5234/$ – see front matter © 2013 Elsevier Masson SAS. All rights reserved.
http://dx.doi.org/10.1016/j.ejmech.2013.09.030

stoichiometric amounts of boron tribromide to obtain compound **6a** (Scheme 1) [12].

Next, compound **4** converted to the corresponding condensation product **7** with benzoyl chloride and acetic anhydride [13,14] (Scheme 2). Fusion reaction converted compound **7** with ammonium acetate to compound **8** [15]. Compounds **9b**–**9d** were synthesized by reaction of the corresponding benzyl bromide with **8** in the presence of sodium hydride and iodomethane, then **6b**–**6d** were prepared by the same step as compound **6a** (Scheme 2). Compounds **10b**–**10d** were obtained by reaction of the corresponding amines with **7** in toluene (Scheme 3). Compounds **11b**–**11d** were prepared by the same step as compound **6a** as shown in Scheme 3.

3. Results and discussion

3.1. Rationale

The previous two-face Bim mimicking compound **1** (Scheme 4) spans from R263 to its opposite pocket (p3) in the BH3 groove of Mcl-1 (Fig. 1a). Especially, the two-face binding mode is conserved upon elaboration of the anthraquinone scaffold. However, previous studies have indicated that tricyclic anthraquinone derivatives may have potential hepatotoxicity and allergic reaction in animal studies [16]. These side effects aroused our interest to simplify the anthraquinone scaffold. The simplification process cannot only help us identify the essential features of this scaffold, but also broaden the scope of the scaffold variations which could serve as the two-face binding mode [17]. In addition, compound **1** loses the mimicking of F69, which is also a hot spot of Bim BH3 α-helix and corresponds to the p4 pocket in the BH3 groove (Fig. 2a) [4]. Previous studies have indicated that p4 occupying could contribute to dual inhibition toward the anti-apoptotic members, such as Bcl-2 and Mcl-1 [18]. As such, we aimed to obtain any new scaffolds providing the base for side chains that could be appended to mimic F69.

As the hydrogen bond formed between the hydroxyl group and R263 in Mcl-1 plays a key role in two-face mimicking [19], we maintained the gallic acid to mimic the hydrophilic residue D67, which is on the opposing helical side of the hydrophobic hotspots. Then, we derived quinazolone and pyrogallol scaffolds (such as compounds **6a** and **11a**) by simplifying ring-C of compound **1** (Scheme 4). Using fluorescence polarization assay (FPA) and computer-aided docking study, we examined whether these scaffolds were the efficient ones to mimic two-face binding mode and maintain dual inhibition of Mcl-1/Bcl-2 proteins.

3.2. Structure-based design, synthesis and evaluation

Firstly, the ring-C of compound **1** was removed, and compound **6a** was obtained (Scheme 4). Docking studies of its lowest energy conformation with Mcl-1 showed that the 2-position and 3-position of **6a** points to the p3 and p4 pockets in Mcl-1, respectively (Fig. 1b). We sought to survey a series of different groups to identify those win appropriate trajectory and length to simultaneously occupy p3 and p4 pockets. We then attached hydrogen atom, methyl and isopropyl groups to the 3-positon, yielding a progressive increase in steric bulk analogues 3-benzyl-6,7,8-trihydroxy-2-phenylquinazolin-4(3H)-one (**6b**), 3-(2-hydroxy-5-methylbenzyl)-6,7,8-trihydroxy-2-phenylquinazolin-4(3H)-one (**6c**), 3-(2-hydroxy-5-isopropylbenzyl)-6,7,8-trihydroxy-2-phenylquinazolin-4(3H)-one (**6d**), respectively (Table 1). A phenyl group was incorporated at the 2-position of the three compounds. The K_i values of these compounds were evaluated using FPA that measured their abilities to competitively displace a Bid-derived peptide from Mcl-1/Bcl-2 as described in the biological assay. R-(−)-Gossypol was used as a positive control. The K_i values of these compounds to Mcl-1/Bcl-2 were outlined in Table 1. We found that replacing hydrogen of **6b** (K_i = 1.214 μM) with a longer methyl (**6c**, K_i = 0.123 μM) resulted in a net 10-fold improvement of affinity. However, a 5-fold decrease of Mcl-1 inhibition was found for compound **6d** (K_i = 0.609 μM), to which a progressively longer isopropyl group was attached.

To illustrate the binding mode of these compounds to Mcl-1 protein, we performed docking studies. Excitingly, compounds **6b**, **6c**, and **6d** could engage into p3 and p4 pockets of Mcl-1 simultaneously. The phenyl group at 2-position indeed mimic F69 of Bim and occupy p4 pocket (Fig. 1c). Notably, an additional hydrogen bond was formed between the hydroxyl of **6c** with T266 of Mcl-1 (Fig. 1d), which could explain the significant increase in the binding affinity. However, the hydrogen bond was not available for **6d** due to the larger isopropyl (Fig. 1e).

The same trend in binding affinity for Bcl-2 was found for these three compounds. **6c** also showed the most potent activity among the three compounds, with a K_i value of 0.179 μM **6b** exhibited a K_i value of 0.959 μM and the value was 1.113 μM for **6d**. The geometry and bulk of the methyl-substitution of benzyl group is proper for occupying Mcl-1 and Bcl-2 proteins.

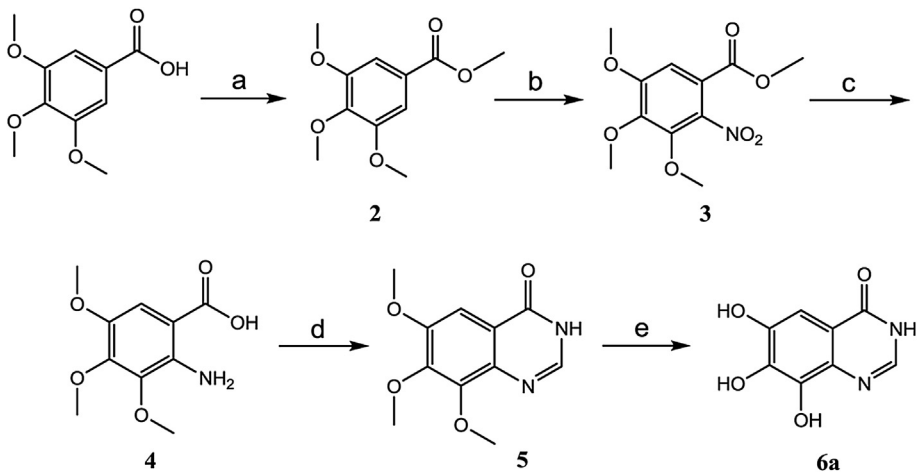

Scheme 1. Reagents and conditions: (a) MeOH, conc. H_2SO_4, reflux; (b) fuming HNO_3, AcOH, ice-bath; (c) $SnCl_2 \cdot 2H_2O$, conc. HCl, reflux; NaOH, EtOH, 45 °C; (d) $HCONH_2$, 130–140 °C, 6 h; (e) BBr_3, CH_2Cl_2, −78 °C − r.t., overnight.

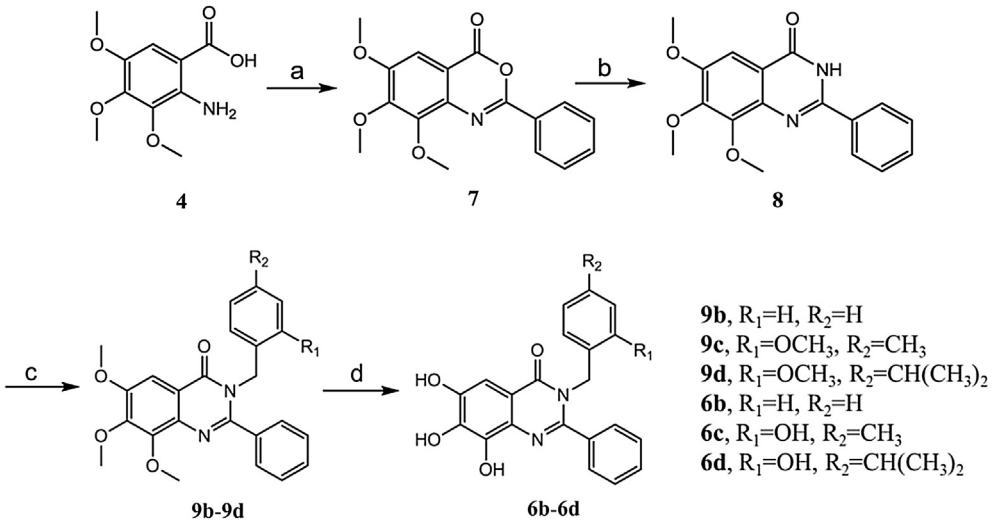

Scheme 2. Reagents and conditions: (a) benzoyl chloride, pyridine, 30 °C; Ac_2O, reflux; (b) NH_4OAc, 170 °C; (c) corresponding benzyl bromide, NaH, KI, CH_2Cl_2; (d) BBr_3, CH_2Cl_2, −78 °C − r.t., overnight.

We tried to further simplify the quinazolone scaffold to identify the most efficient scaffold for two-face Bim mimicry. We designed one phenyl ring possessing three adjacent hydroxyl groups as the next scaffold (Scheme 1). Based on the pyrogallol scaffold, a series of compounds 2-benzamido-N-butyl-3,4,5-trihydroxybenzamide (**11b**), 2-benzamido-N-benzyl-3,4,5-trihydroxybenzamide (**11c**), and 2-benzamido-3,4,5-trihydroxy-N-(3-phenylpropyl) benzamide (**11d**) were explored. In these compounds, benzamide groups and flexible amide bonds were employed to occupy p3 and p4 pockets. However, the FPA indicated that the all three compounds showed affinities in the μM range toward Bcl-2 (K_i = 1.925, 1.323 and 8.040 μM, respectively) and Mcl-1 proteins (K_i = 1.981, 2.816 and 3.240 μM, respectively), which were lower than compound **1**, shown in Table 1. The reason might be the free rotation between the side chains and the pyrogallol scaffold resulting in multiple conformations. As such, disfavored changes in conformational entropy are required for these molecules to bind to the BH3 groove, which lead to entropic penalties that negatively impact binding energy [20,21]. The lack of sufficient rigidity of the derivatives of pyrogallol may result in the failure of mimicking the two-face of α-helix and suboptimal affinities for the targets.

From the data mentioned above, the quinazolone scaffold was successfully applied to the design of two-face Bim mimetics (Fig. 2b). A rigid bicyclic ring was necessary and efficient to maintain the two-faced binding mode.

4. Conclusions

In summary, a novel dual inhibitor **6c** [6,7,8-trihydroxy-3-(2-hydroxy-5-methylbenzyl)-2-phenylquinazolin-4(3H)-one] was obtained, which exhibited K_i values of 0.123 μM for Mcl-1 and 0.179 μM for Bcl-2. It was inferred that the rigid quinazolone scaffold is necessary and efficient to maintain the two-face binding mode by mimicking the hydrophilic residue D67 of Bim BH3 α-helix and occupying the hydrophobic p3 and p4 pocket of Mcl-1/Bcl-2. We expect these results could provide some fundamental insights into the future design and development of Bim BH3 α-helix mimetics.

5. Experimental section

5.1. Chemistry

5.1.1. Materials and methods

All commercial reagents were purchased and used without further purification or distillation unless otherwise stated. Melting points were measured on a Griffin apparatus and are uncorrected. NMR spectra were recorded with Bruker AV-400 spectrometer with chemical shifts reported as parts per million (in DMSO, TMS as internal standard). The following abbreviations are used for multiplicity of NMR signals: s = singlet, d = doublet, t = triplet, q = quartet, m = multiplet. High-resolution mass spectra (HRMS) were obtained on HPLC-Q-T of MS (Micro) spectrometer. Column chromatography was performed on silica gel 200–300 mesh. Purity of all final products was determined by analytical HPLC to be ≥95%. HPLC purity of compounds was measured with a reverse phase HPLC (XBridge C18, 4.6 × 150 mm, 5 μm) with two diverse wavelength detection systems.

5.1.2. Methyl-3,4,5-trimethoxybenzoate (*2*)

3,4,5-trimethoxybenzoic acid (10 g, 47 mmol) was dissolved in 30 mL methanol. When complete solution was obtained, 2.5 mL concentrated sulphuric acid was incrementally added over 30 min at room temperature.

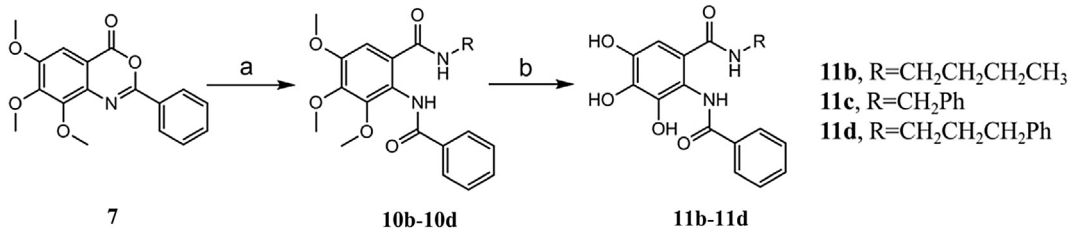

Scheme 3. Reagents and conditions: (a) corresponding amine, toluene, reflux; (b) BBr_3, CH_2Cl_2, −78 °C − r.t., overnight.

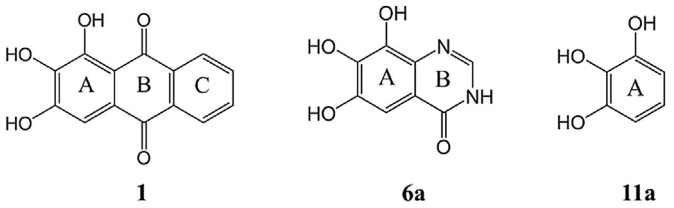

Scheme 4. The scaffolds simplification process.

Then the reaction mixture was heated under reflux for 8 h maintaining anhydrous conditions by use of a $CaCl_2$ drying tube attached to the condenser. After cooled to room temperature, the resulting white needle crystal was filtered and used in the next step without further disposal, yield 93.5%; mp 75–76 °C. ^{1}H NMR (400 MHz, DMSO-d_6) δ: 7.14 (s, 2H, PhH), 3.90–3.85 (t, 9H, $3OCH_3$), 3.83 (s, 3H, $COOCH_3$). ^{13}C NMR (DMSO-d_6) δ: 165.92, 153.11, 153.07, 143.52, 126.43, 106.42, 106.21, 60.87, 56.92, 56.23, 51.55. TOF MS (EI^+): $C_{11}H_{14}O_5$, calcd for 226.0357, found 226.0355.

5.1.3. *Methyl-2-nitro-3,4,5-trimethoxybenzoate (**3**)*

To a stirred solution of methyl-3,4,5-trimethoxybenzoate (**2**) (6.0 g, 26.5 mmol) in AcOH (20 mL), fuming HNO_3 (6.5 mL) was added carefully during 1 h in ice-bath. After addition of the acid, the solution was allowed to be stirred for 1–2 h at room temperature. The reaction mixture was then poured into ice water (60 mL). The resulting precipitate was filtered, washed with water, dried and recrystallized from EtOH–H_2O (2:1, V:V). Pale yellow needle crystal, yield 30.4%; mp 62–63 °C. ^{1}H NMR (400 MHz, DMSO-d_6) δ: 7.34 (s, 1H, PhH), 3.94–3.89 (*t*, 9H, $3OCH_3$), 3.83 (s, 3H, $COOCH_3$). ^{13}C NMR (DMSO-d_6) δ: 163.31, 154.75, 146.29, 145.51, 139.64, 117.72, 109.28, 63.11, 61.62, 57.19, 53.75. TOF MS (EI^+): $C_{11}H_{13}NO_7$, calcd for 271.0723, found 271.0725.

5.1.4. *2-Amino-3,4,5-trimethoxybenzoic acid (**4**)*

A mixture of powder $SnCl_2{\cdot}2H_2O$ (5.3 g, 23.5 mmol) and 95% ethanol solution (15 mL) was stirred for 0.5–1 h at room temperature until most solid was dissolved. Then methyl-2-nitro-3,4,5-trimethoxybenzoate (**3**) (1.12 g, 4.13 mmol) and concentrated hydrochloric acid (8 mL) were added to the solution. The reaction mixture was carefully heated to reflux under nitrogen, and maintained the temperature for 30–40 min. The reaction mixture was cooled by ice-bath and stirred for 10 min. The precipitated complex stannic double salt was filtered, washed with little concentrated hydrochloric acid. The resulting mixture was dissolved in 100 mL 10% K_2CO_3 solution, adjusted to pH 9–10 and extracted with CH_2Cl_2. The evaporated substrate was methyl 2-nitro-3,4,5-trimethoxy-benzoate. A stirred solution of methyl 2-nitro-3,4,5-trimethoxybenzoate (1.0 g, 4 mmol) in 1 mol/L NaOH (15 mL, 15 mmol) and 95% EtOH (15 mL) was heated at 45–50 °C in water bath for 2 h, and the reaction mixture was cooled by ice-water. The ethanol solvent need to evaporate under rotary evaporation apparatus. Then, acetic acid was added dropwise with stirring while maintaining the temperature below 20 °C. The mixture was adjusted to pH 5–6. The solid was filtered, washed with water, and recrystallized from EtOH. Pale yellow needles crystal, yield 61.9%; mp 138–139 °C. ^{1}H NMR (400 MHz, DMSO-d_6) δ: 11.05 (s, 1H, COOH), 6.76 (s, 2H, NH_2), 7.06 (s, 1H, PhH), 3.93–3.85 (t, 9H, $3OCH_3$). ^{13}C NMR (DMSO-d_6) δ: 169.45, 147.62, 142.93, 141.61, 140.47, 109.33, 104.52, 60.91, 60.66, 56.63. TOF MS (EI^+): $C_{10}H_{13}NO_5$, calcd for 227.0618, found 227.0615.

5.1.5. *6,7,8-Trihydroxyquinazolin-4(3H)-one (**5**)*

A mixture of 1.1 g (5 mmol) 2-amino-3,4,5-trimethoxybenzoic acid (**4**) and excess of formamide (4 mL) was stirred for 5 h at 130–140 °C. After the reaction was over, a suitable water (about 5 mL) was dropwise to the reaction mixture to resolve the excess of formamide at 100 °C. The resulting gray solid was filtered, washed with water and recrystallized from EtOH. Pale brown crystal, yield 55.4%; mp 220–222 °C. ^{1}H NMR (400 MHz, DMSO-d_6) δ: 12.21 (s, 1H, NH), 8.01 (s, 1H, Ar–H), 7.35 (s, 1H, Ar–H), 3.95–3.88 (t, 9H, $3OCH_3$). TOF MS (EI^+): $C_{11}H_{12}N_2O_4$, calcd for 236.0418, found 236.0415.

5.1.6. *6,7,8-Trimethoxy-2-phenyl-4H-benzo[d] [1,3]oxazin-4-one (**7**)*

A stirred solution of 2-amino-3,4,5-trimethoxybenzoic acid (**4**) (416 mg, 1.83 mmol) in dry pyridine (10 mL) was treated dropwise

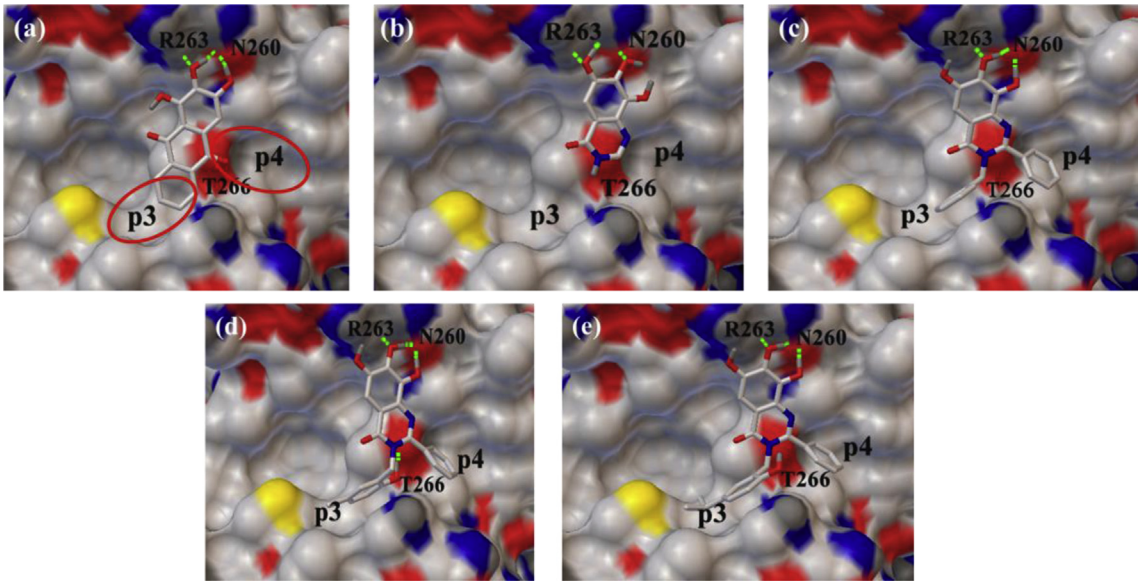

Fig. 1. Predicted binding models of Mcl-1 in complex with (a) **1**, (b) **6a**, (c) **6b**, (d) **6c** and (e) **6d**. Mcl-1 is shown in a surface representation, and the carbon, oxygen, nitrogen, and sulfur atoms are shown in gray, red, blue, and yellow, respectively. The p3, p4 pockets and some residues are labeled. Hydrogen bonds are depicted as dotted lines in green. (For interpretation of the references to colour in this figure legend, the reader is referred to the web version of this article.)

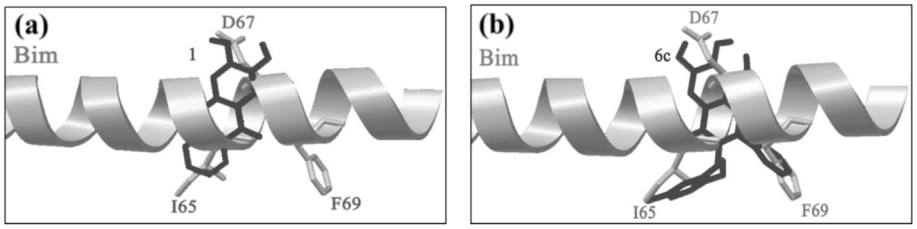

Fig. 2. (a) The resultant overlay of compound **1** (dark gray) on the Bim BH3 peptide (light gray) is displayed. (b) The resultant overlay of compound **6c** (dark gray) on the Bim BH3 peptide (light gray) is displayed.

with benzoyl chloride (500 μL). The mixture was stirred at 30 °C for 6 h and poured onto a mixture of ice and hydrochloric acid. The obtained residue was washed with water, recrystallized from ethanol as light pink solid. A suspension of this solid (573 mg) in acetic anhydride (20 mL) was heated under reflux (4 h) and then concentrated. The residue was crystallized from ethanol, giving 6,7,8-trimethoxy-2-phenyl-4H-benzo[d][1,3]oxazin-4-one (**5**) (450 mg, 78.6% overall) as dark yellow crystals, mp 170–171 °C. ^{1}H NMR (400 MHz, DMSO-d_6) δ: 8.17–8.19 (d, J = 8.4 H z, 2H, Ar–H), 7.59–7.67 (m, 3H, Ar–H), 7.39 (s, 1H, Ar–H), 3.93–4.09 (t, 9H, 3OCH$_3$). ^{13}C NMR (DMSO-d_6) δ: 159.44, 156.32, 151.53, 145.92, 145.23, 133.21, 131.02, 129.85, 128.83, 128.41, 128.12, 127.93, 110.53, 99.31, 60.82, 56.16, 55.76. TOF MS (EI$^+$): $C_{17}H_{15}NO_5$, calcd for 313.0818, found 313.0816.

*5.1.7. 6,7,8-Trimethoxy-2-phenylquinazolin-4(3H)-one (**8**)*

6,7,8-trimethoxy-2-phenyl-4H-benzo[d][1,3]oxazin-4-one (**7**) (100 mg, 0.32 mmol) was stirred with ammonium acetate (2.5 g, 32 mmol) at 170 °C for 1 h under nitrogen. After cooling to 50 °C, the solution was diluted with hot methanol (3 mL). The resultant solution was stirred under reflux for 1 h, cooled to room temperature. The resulting solid was filtered and rinsed with methanol and dried. White solid was obtained yield 80%; mp 247–248 °C. ^{1}H NMR (400 MHz, DMSO-d_6) δ: 8.36 (d, J = 8.4 Hz, 2H, Ar–H), 7.86–7.88 (m, 3H, Ar–H), 7.28 (s, 1H, Ar–H), 5.88 (s, 1H, NH), 4.33–4.37 (t, 9H, OCH$_3$). ^{13}C NMR (DMSO-d_6) δ: 161.08, 152.32, 151.73, 146.67, 143.95, 132.52, 131.43, 130.45, 128.96, 128.32, 128.12, 127.54, 111.73, 101.52, 60.82, 57.34, 56.76. TOF MS (EI$^+$): $C_{17}H_{16}N_2O_4$, calcd for 312.0678, found 312.0679.

*5.1.8. General procedure for the preparation of **9b**–**9d***

A stirred solution of 6,7,8-trimethoxy-2-phenylquinazolin-4(3H)-one (**8**) (200 mg, 0.641 mmol) in 10 mL of DMF was added sodium hydride (10 mmol) under nitrogen at room temperature. After stirring for 1 h, corresponding benzyl bromide (3 mmol) and iodomethane were added and the reaction mixture was further stirred for 1–1.5 h under nitrogen. After pouring the mixture into water slowly, standing for 1 h, the residue was filtered, recrystallized from EtOH as the final compounds.

*5.1.8.1. 3-Benzyl-6,7,8-trimethoxy-2-phenylquinazolin-4(3H)-one (**9b**).* Yield: 150 mg, 58.2%. ^{1}H NMR (400 MHz, DMSO-d_6) δ: 8.11 (d, J = 8.4 Hz, 2H, Ar–H), 7.96–7.98 (m, 3H, Ar–H), 7.63 (s, 1H, Ar–H), 7.37–7.39 (d, J = 8.4 Hz, 2H, Ar–H), 7.09–7.11 (m, 3H, Ar–H), 5.61 (s, 2H, CH$_2$), 4.21–4.23 (t, 9H, OCH$_3$). ^{13}C NMR (DMSO-d_6) δ: 163.61, 156.25, 151.76, 147.34, 143.95, 136.57, 131.56, 130.47, 129.76, 129.01, 128.85, 128.67, 128.45, 128.21, 127.98, 127.75, 127.44, 127.03, 117.64, 101.23, 61.23, 57.82, 56.34, 46.12. TOF MS (EI$^+$): $C_{24}H_{22}N_2O_4$, calcd for 402.0423, found 402.0426.

*5.1.8.2. 6,7,8-Trimethoxy-3-(2-methoxy-5-methylbenzyl)-2-phenylquinazolin-4(3H)-one (**9c**).* Yield: 101 mg, 35.3%. ^{1}H NMR (400 MHz, DMSO-d_6) δ: 8.51 (d, J = 8.4 Hz, 2H, Ar–H), 8.16–8.18 (m, 3H, Ar–H), 7.84–7.86 (d, J = 8.4 Hz, 2H, Ar–H), 7.59–7.61 (s, 1H, Ar–H), 7.17 (s, 1H, Ar–H), 5.37 (d, 2H, CH$_2$), 4.01–4.03 (m, 12H, OCH$_3$), 2.37 (s, 3H, CH$_3$). ^{13}C NMR (DMSO-d_6) δ: 165.64, 156.34, 153.76, 151.72, 146.85, 144.34, 138.52, 131.43, 130.57, 129.51, 129.08, 128.53, 128.23, 128.01, 127.75, 125.93, 121.43, 116.78, 115.32, 101.64, 61.92, 58.23, 56.78, 56.32, 39.87, 21.67. TOF MS (EI$^+$): $C_{26}H_{26}N_2O_5$, calcd for 446.0243, found 446.0241.

*5.1.8.3. 3-(5-isopropyl-2-methoxybenzyl)-6,7,8-trimethoxy-2-phenylquinazolin-4(3H)-one (**9d**).* Yield: 85 mg, 28.0%. ^{1}H NMR (400 MHz, DMSO-d_6) δ: 7.95–7.97 (d, J = 8.4 Hz, 2H, Ar–H), 7.67–7.69 (m, 3H, Ar–H), 7.32–7.34 (d, J = 8.4 Hz, 2H, Ar–H), 7.07–7.09 (s,1H, Ar–H), 6.79 (s, 1H, Ar–H), 5.39 (s, 2H, CH$_2$), 4.24–4.28 (m, 12H, OCH$_3$), 2.93 (m, 1H, CH), 1.76 (d, 6H, 2CH$_3$). ^{13}C NMR (DMSO-d_6) δ: 161.62, 156.35, 153.67, 151.76, 149.43, 146.13, 143.97, 130.45, 130.34, 129.34, 129.03, 128.75, 128.42, 128.12, 127.56, 126.15, 118.54, 115.12, 113.15,101.23, 62.13, 58.11, 57.34, 56.89, 39.34, 33.55, 23.56, 23.12. TOF MS (EI$^+$): $C_{28}H_{30}N_2O_5$, calcd for 474.0253, found 474.0256.

*5.1.9. General procedure for the preparation of **10b**–**10d***

A stirred solution of 6,7,8-trimethoxy-2-phenyl-4H-benzo[d][1,3]oxazin-4-one (**7**) (90 mg, 0.287 mmol) in 5 mL of toluene was added corresponding amine (0.733 mmol), and the reaction mixture was heated under reflux for 4–5 h. After cooling down, the residue was filtered, recrystallized from ethanol as the final compound.

*5.1.9.1. 2-Benzamido-N-butyl-3,4,5-trimethoxybenzamide (**10b**).* Yield: 49 mg, 44.2%. ^{1}H NMR (400 MHz, DMSO-d_6) δ: 8.26 (s, 1H, NH), 8.11 (d, J = 8.4 Hz, 2H, Ar–H), 7.96–7.98 (m, 3H, Ar–H), 7.43 (s, 1H, Ar–H), 5.58 (s, 1H, NH), 4.21–4.23 (t, 9H, OCH$_3$), 3.89 (m, 2H, CH$_2$), 1.65–1.67 (m, 4H, CH$_2$CH$_2$), 1.12 (t, 3H, CH$_3$). ^{13}C NMR (DMSO-d_6) δ: 170.32, 164.76, 148.82, 142.87, 141.23, 134.25, 132.11, 128.76, 128.23, 127.53, 127.11, 120.32, 117.34, 105.35, 60.82, 60.24, 56.12, 39.42, 32.21, 19.86, 13.34. TOF MS (EI$^+$): $C_{21}H_{26}N_2O_5$, calcd for 386.0423, found 386.0426.

*5.1.9.2. 2-Benzamido-N-benzyl-3,4,5-trimethoxybenzamide (**10c**).* Yield: 55 mg, 45.6%. ^{1}H NMR (400 MHz, DMSO-d_6) δ: 8.53 (s, 1H, NH), 8.11 (s, 1H, NH), 7.94–7.96 (d, J = 8.4 Hz, 2H, Ar–H), 7.59–7.61 (m,3H, Ar–H), 7.37–7.39 (d, J = 8.4 Hz, 2H, Ar–H), 7.09–7.11 (m,3H, Ar–H), 6.89 (s, 1H, Ar–H), 4.37 (d, 2H, CH$_2$), 4.01–4.03 (t, 9H, OCH$_3$). ^{13}C NMR (DMSO-d_6) δ: 167.86, 164.71, 148.83, 142.92, 142.45, 137.96, 134.26, 132.13, 128.92, 128.42, 128.11, 128.02, 127.68, 127.43, 126.97, 126.57, 126.01, 120.34, 117.23, 101.69, 60.91, 60.53, 56.15, 44.78. TOF MS (EI$^+$): $C_{24}H_{24}N_2O_5$, calcd for 420.0243, found 420.0241.

*5.1.9.3. 2-Benzamido-3,4,5-trimethoxy-N-(3-phenylpropyl)benzamide (**10d**).* Yield: 85 mg, 72.9%. ^{1}H NMR (400 MHz, DMSO-d_6) δ: 8.23 (s, 1H, NH), 7.95–7.97 (d, J = 8.4 Hz, 2H, Ar–H), 7.67–7.69 (m,3H, Ar–H), 7.32–7.34 (d, J = 8.4 Hz, 2H, Ar–H), 7.07–7.09 (m,3H, Ar–H), 6.79 (s, 1H, Ar–H), 6.07 (s, 1H, NH), 4.24–4.28 (t, 9H, OCH$_3$),

Table 1
Binding affinities (by FPA) of compounds to Mcl-1/Bcl-2.

Compounds	Structures	K_i[a] ± SD (μM)	
		Mcl-1	Bcl-2
1	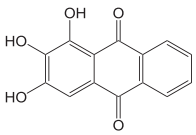	1.211 ± 0.036	1.325 ± 0.027
6a	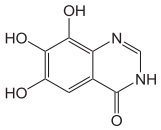	5.981 ± 0.012	9.282 ± 0.023
6b	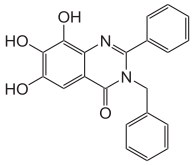	1.214 ± 0.038	0.959 ± 0.021
6c	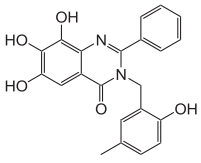	0.123 ± 0.006	0.179 ± 0.009
6d	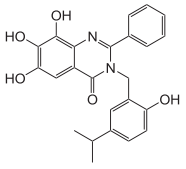	0.609 ± 0.012	1.113 ± 0.025
11b	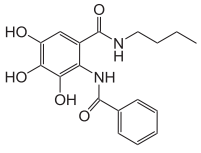	1.981 ± 0.014	1.925 ± 0.056
11c	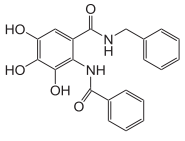	2.816 ± 0.037	1.323 ± 0.028
11d	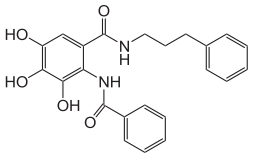	3.240 ± 0.048	8.040 ± 0.109
(−)-Gossypol	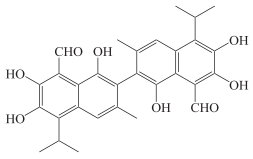	0.190 ± 0.005	0.558 ± 0.012

[a] Values were measured by FPA for inhibition constant (K_i). The values are the mean ± SD of three independent experiments.

3.96 (m, 2H, CH_2), 2.96 (m, 2H, CH_2), 1.89 (m, 2H, CH_2). ^{13}C NMR (DMSO-d_6) δ: 174.31, 169.32, 152.36, 145.78, 142.38, 141.26, 136.28, 132.15, 129.54, 129.11, 128.87, 128.46, 128.21, 127.86, 127.52, 126.84, 126.02, 121.33, 119.35, 101.62, 61.89, 60.94, 57.82, 40.64, 32.11, 29.81. TOF MS (EI^+): $C_{26}H_{28}N_2O_5$, calcd for 448.0253, found 448.0256.

*5.1.10. General procedure for the preparation of **6a–6d**, **11b–11d***

*5.1.10.1. 6,7,8-Trihydroxy-2-phenyl-4H-benzo[d][1,3]oxazin-4-one (**6a**).* In this step, all reagents and reactors are required to be anhydrous. 6,7,8-trihydroxyquinazolin-4(3H)-one (**5**) (50.5 mg, 0.214 mmol) in 5 mL of anhydrous CH_2Cl_2 was placed in a flask under liquid nitrogen condition. Then boron tribromide (320 μL, 3.3 mmol) in CH_2Cl_2 (5 mL) was slowly added at ultralow temperature and the solution was stirred for the time and temperature slowly returned to room temperature. After reacting overnight, methanol (1 mL) was added. The mixture was stirred for another 15 min after adding additional H_2O (1 mL). The solid was filtered, washed with water, recrystallized from ethanol- H_2O as yellow solid, yield 61.9%. ^{1}H NMR (400 MHz, DMSO-d_6) δ: 9.76 (s, 1H, OH), 9.56 (s, 1H, OH), 9.43 (s, 1H, OH), 8.19 (s, 1H, Ar–H), 7.39 (s, 1H, Ar–H). TOF MS (EI^+): $C_8H_6N_2O_4$, calcd for 194.0423, found 194.0425.

The step to obtain **6b–6d**, **11b–11d** is same with the process of compound **6a**. The starting material is 100 mg separately.

*5.1.10.2. 3-Benzyl-6,7,8-trihydroxy-2-phenylquinazolin-4(3H)-one (**6b**).* Yield: 33 mg, 36.8%. ^{1}H NMR (400 MHz, DMSO-d_6) δ: 10.65 (s, 1H, OH), 10.24 (s, 1H, OH), 9.98 (s, 1H, OH), 8.21–8.23 (d, J = 8.4 Hz, 2H, Ar–H), 7.96–7.98 (m,3H, Ar–H), 7.43–7.45 (d, J = 8.4 Hz, 2H, Ar–H), 7.11–7.13 (m,3H, Ar–H), 6.93 (s, 1H, Ar–H), 5.89 (s, 2H, CH_2). ^{13}C NMR (DMSO-d_6) δ: 164.61, 155.25, 151.76, 149.34, 146.95, 139.57, 131.56, 130.47, 129.76, 129.01, 128.85, 128.67, 128.45, 128.21, 127.98, 127.75, 127.44, 127.03, 117.64, 109.23, 46.67. TOF MS (EI^+): $C_{21}H_{16}N_2O_4$, calcd for 360.0223, found 360.0225.

*5.1.10.3. 6,7,8-Trihydroxy-3-(2-hydroxy-5-methylbenzyl)-2-phenylquinazolin-4(3H)-one (**6c**).* Yield: 23 mg, 26.3%. ^{1}H NMR (400 MHz, DMSO-d_6) δ: 11.05 (s, 1H, OH), 10.76 (s, 1H, OH), 10.43 (s, 1H, OH), 10.12 (s, 1H, OH), 8.16–8.18 (d, J = 8.4 Hz, 2H, Ar–H), 7.69–7.71 (m,3H, Ar–H), 7.45–7.47 (d, J = 8.4 Hz, 2H, Ar–H), 7.19 (s,1H, Ar–H), 6.99 (s, 1H, Ar–H), 5.09 (s, 2H, CH_2), 2.37 (s, 3H, CH_3). ^{13}C NMR (DMSO-d_6) δ: 163.64, 157.34, 153.46, 151.78, 146.81, 144.74, 138.32, 131.43, 130.67, 129.51, 129.08, 128.53, 128.23, 128.01, 127.75, 125.93, 121.43, 116.78, 115.32, 107.64, 39.87, 21.67. TOF MS (EI^+): $C_{22}H_{18}N_2O_5$, calcd for 390.0243, found 390.0241.

*5.1.10.4. 6,7,8-Trihydroxy-3-(2-hydroxy-5-isopropylbenzyl)-2-phenylquinazolin-4(3H)-one (**6d**).* Yield: 19 mg, 21.5%. ^{1}H NMR (400 MHz, DMSO-d_6) δ: 11.23 (s, 1H, OH), 10.69 (s, 1H, OH), 10.27 (s, 1H, OH), 9.89 (s, 1H, OH), 8.43–8.45 (d, J = 8.4 Hz, 2H, Ar–H), 7.96–7.98 (m,3H, Ar–H), 7.62–7.64 (d, J = 8.4 Hz, 2H, Ar–H), 7.21 (s,1H, Ar–H), 7.08 (s, 1H, Ar–H), 5.22 (s, 2H, CH_2), 2.76 (m, 1H, CH), 1.96 (d, 6H, $2CH_3$). ^{13}C NMR (DMSO-d_6) δ: 163.62, 157.35, 153.87, 151.76, 149.43, 143.13, 139.97, 130.45, 130.34, 129.34, 129.03, 128.75, 128.42, 128.12, 127.56, 126.15, 118.54, 117.12, 116.15,113.23, 39.23, 33.55, 23.43, 23.12. TOF MS (EI^+): $C_{24}H_{22}N_2O_5$, calcd for 418.0578, found 418.0576.

*5.1.10.5. 2-Benzamido-N-butyl-3,4,5-trihydroxybenzamide (**11b**).* Yield: 40 mg, 44.9%. ^{1}H NMR (400 MHz, DMSO-d_6) δ: 10.65 (s, 1H, OH), 10.24 (s, 1H, OH), 9.98 (s, 1H, OH), 8.45(s, 1H, NH), 8.21–8.23 (d, J = 8.4 Hz, 2H, Ar–H), 7.96–7.98 (m,3H, Ar–H), 7.43 (s, 1H, Ar–H), 5.58 (s, 1H, NH), 3.89 (m, 2H, CH_2), 1.65–1.67 (m, 4H, CH_2CH_2), 1.12 (t, 3H, CH_3). ^{13}C NMR (DMSO-d_6) δ: 170.32, 164.76, 143.82, 141.87, 139.23, 134.67, 132.51, 128.78, 128.33, 127.67, 127.21, 122.32, 118.34,

107.35, 39.22, 32.43, 19.54, 13.84. TOF MS (EI^+): $C_{18}H_{20}N_2O_5$, calcd for 344.1423, found 344.1425.

*5.1.10.6. 2-Benzamido-N-benzyl-3,4,5-trihydroxybenzamide (**11c**).* Yield: 37 mg, 41.1%. ^1H NMR (400 MHz, DMSO-d_6) δ: 10.76 (s, 1H, OH), 10.43 (s, 1H, OH), 10.12 (s, 1H, OH), 8.77 (s, 1H, NH), 8.58 (s, 1H, NH), 8.12–8.14 (d, J = 8.4 Hz, 2H, Ar–H), 7.69–7.71 (m,3H, Ar–H), 7.43–7.45 (d, J = 8.4 Hz, 2H, Ar–H), 7.12–7.14 (m,3H, Ar–H), 6.99 (s, 1H, Ar–H), 4.37 (d, 2H, CH_2). ^{13}C NMR (DMSO-d_6) δ: 167.93, 164.51, 144.83, 141.92, 140.45, 138.96, 134.16, 132.43, 128.92, 128.42, 128.11, 128.02, 127.89, 127.43, 126.97, 126.57, 126.01, 122.34, 118.23, 107.69, 44.18. TOF MS (EI^+): $C_{21}H_{18}N_2O_5$, calcd for 378.1243, found 378.1241.

*5.1.10.7. 2-Benzamido-3,4,5-trihydroxy-N-(3-phenylpropyl)benzamide (**11d**).* Yield: 35 mg, 38.6%. ^1H NMR (400 MHz, DMSO-d_6) δ: 10.43 (s, 1H, OH), 10.09 (s, 1H, OH), 9.76 (s, 1H, OH), 8.53 (s, 1H, NH), 8.04–8.06 (d, J = 8.4 Hz, 2H, Ar–H), 7.86–7.88 (m,3H, Ar–H), 7.62–7.64 (d, J = 8.4 Hz, 2H, Ar–H), 7.21–7.23 (m,3H, Ar–H), 7.08 (s, 1H, Ar–H), 6.44 (s, 1H, NH), 3.96 (m, 2H, CH_2), 2.96(m, 2H, CH_2), 1.89 (m, 2H, CH_2). ^{13}C NMR (DMSO-d_6) δ: 176.31, 169.12, 153.36, 148.78, 141.38, 140.26, 137.28, 133.35, 129.58, 129.11, 128.87, 128.46, 128.21, 127.86, 127.52, 126.54, 126.02, 121.33, 117.35, 106.62, 40.64, 32.11, 28.81. TOF MS (EI^+): $C_{23}H_{22}N_2O_5$, calcd for 406.1578, found 406.1576.

5.2. Binding affinity assay

5.2.1. Reagents

A 21-residue Bid BH3 peptide (residues 79–99) [22] bearing a 6-carboxy-fluorescein succinimidyl ester fluorescence tag (FAM-Bid) was synthesized at HD Biosciences (Shanghai, China) [23]. Recombinant proteins of Bcl-2 and Mcl-1 were synthesized and purified from bacteria of *Escherichia coli* BL21 as described in our previous study [18].

5.2.2. Fluorescence polarization-based binding assay (FPA)

For the competitive binding assay for Bcl-2 protein, FAM-Bid peptide (20 nM) and Bcl-2 protein (660 nM) were preincubated in the assay buffer (100 mM potassium phosphate, pH 7.5; 100 mg/mL bovine gamma globulin; 0.02% sodium azide) for 2 min. Each inhibitor was first dissolved in pure DMSO to obtain a 10 mM stock solution. Then the stock solution was diluted successively to get the solution with different concentration gradients (1000 μM, 100 μM, 10 μM, 1 μM, 0.1 μM). Next, serial dilutions of compounds were added. After 10 min incubation, the polarization values were measured using the Spectra Max M5 Detection System in a black 96-well plate. Saturation experiments determined that FAM-Bid binds to the Bcl-2 protein with a K_d value of 125 nM. For Mcl-1, assays were performed in the same manner as that for Bcl-2 with the following exceptions: 55 nM Mcl-1 and 20 nM FAM-Bid peptide were used in the assay buffer (25 mM Tris, pH 8.0; 150 mM NaCl). FAM-Bid peptide binds to the Mcl-1 protein with a K_d value of 13 nM (−)-Gossypol was used as comparison in our assay. The K_i value for each inhibitor was calculated using the equation Wang et al. have developed for FP-based assays. The computer program for calculating K_i values for FP-based assays are available free of charge at: http://sw16.im.med.umich.edu/software/calc_ki/ [18].

5.3. Molecular docking

The 3D structures of Mcl-1 (Mcl-1; PDB ID: 2NL9) was obtained from the protein bank in the RCSB [24]. The mol2 structures of the inhibitors were generated using Chembio3D Ultra 11.0 followed by energy minimization. AutoDock 4.2 program equipped with ADT was used to perform the automated molecular docking [25]. Grid maps covering residues that were perturbed more than the threshold value of 0.1 ppm in the binding groove of the proteins were defined for all inhibitors in the AutoDock calculations using a grid spacing about of 0.375 Å. For each docking job, 1000 hybrid GA-LS runs were carried-out. A total of 1000 possible binding conformations were generated and grouped into clusters based on a 1.0 Å cluster tolerance. The docking models were analyzed and represented using ADT.

Acknowledgments

This work was supported by the National Natural Science Foundation of China (21372036).

Appendix A. Supplementary data

Supplementary data associated with this article can be found in the online version, at http://dx.doi.org/10.1016/j.ejmech.2013.09.030. These data include MOL files and InChiKeys of the most important compounds described in this article.

References

[1] A. Degterev, M. Boyce, J. Yuan, The channel of death, J. Cell Biol. 155 (2001) 695–698.
[2] G. Tang, Z. Nikolovska-Coleska, S. Qiu, C. Yang, J. Guo, S. Wang, Acylpyrogallols as inhibitors of antiapoptotic Bcl-2 proteins, J. Med. Chem. 51 (2008) 717–720.
[3] L.D. Walensky, A.L. Kung, I. Escher, T.J. Malia, S. Barbuto, R.D. Wright, G. Wagner, G.L. Verdine, S.J. Korsmeyer, Activation of apoptosis in vivo by a hydrocarbon-stapled BH3 helix, Science 305 (2004) 1466–1470.
[4] P.E. Czabotar, E.F. Lee, M.F. van Delft, C.L. Day, B.J. Smith, D.C.S. Huang, W.D. Fairlie, M.G. Hinds, P.M. Colman, Structural insights into the degradation of Mcl-1, Proc. Natl. Acad. Sci. U. S. A. 104 (2007) 6217–6222.
[5] Z. Zhang, H. Yang, G. Wu, Z. Li, T. Song, X.Q. Li, Probing the difference between BH3 groove of Mcl-1 and Bcl-2 protein: Implications for dual inhibitors design, Eur. J. Med. Chem. 46 (2011) 3909–3916.
[6] L. Chen, S.N. Willis, A. Wei, B.J. Smith, J.I. Fletcher, M.G. Hinds, P.M. Colman, C.L. Day, J.M. Adams, D.C. Huang, Differential targeting of prosurvival Bcl-2 proteins by their BH3-only ligands allows complementary apoptotic function, Mol. Cell 17 (2005) 393–403.
[7] Z. Zhang, X. Li, T. Song, Y. Zhao, Y. Feng, An anthraquinone scaffold for putative, two-face Bim BH3 α-helix mimic, J. Med. Chem. 55 (2012) 10735–10741.
[8] B.N. Bullock, A.L. Jochim, P.S. Arora, Assessing helical protein interfaces for inhibitor design, J. Am. Chem. Soc. 133 (2011) 14220–14223.
[9] E.F. Lee, P.E. Czabotar, B.J. Smith, K. Deshayes, K. Zobel, P.M. Colman, W.D. Fairlie, Crystal structure of ABT-737 complexed with Bcl-xL: implications for selectivity of antagonists of the Bcl-2 family, Cell Death Differ. 14 (2007) 1711–1713.
[10] H. Yin, G. Lee, K.A. Sedey, O. Kutzki, H.S. Park, B.P. Orner, J.T. Ernst, H. Wang, A.D. Hamilton, Synthetic inhibitors of extended helix–protein interactions, J. Am. Chem. Soc. 127 (2005) 10191–10196.
[11] G. Liu, L. Sun, C. Liu, C. Ji, Q. Wen, S. Ma, Microwave assisted synthesis of novel 6,7,8-Trimethoxy N- substituted- 4- amino quinazoline compounds, J. Heterocycl. Chem. 45 (2008) 759–764.
[12] S. Punna, S. Meunier, M.G. Finn, A hierarchy of aryloxide deprotection, Org. Lett. 6 (2004) 2777–2779.
[13] A.K. Tiwari, V.K. Singh, A. Bajpai, G. Shukla, S. Singh, A.K. Mishra, Synthesis and biological properties of 4-(3H)-quinazolone derivatives, Eur. J. Med. Chem. 42 (2007) 1234–1238.
[14] J.B. Jiang, B.A. Dusak, D.L. Dexter, G.J. Kang, E. Hamel, Synthesis and biological evaluation of 2-styrylquinazolin-4(3H)-ones, a new class of antimitotic anticancer agents which inhibit tubulin polymerization, J. Med. Chem. 33 (1990) 1721–1728.
[15] A.A. Laeva, E.V. Nosova, G.N. Lipunova, A.V. Golovchenko, N.Y. Adonin, V.N. Parmon, V.N. Charushin, Fluorine-containing heterocycles: XIX. synthesis of fluorine-containing quinazolin-4-ones from 3,1-benzoxazin-4-ones, Russ. J. Org. Chem. 45 (2009) 913–920.
[16] J.H. Xing, E.E. Soffer, Adverse effects of laxatives, Dis. Colon Rectum 44 (2001) 1201–1209.
[17] Y. Dong, Q. Shi, K. Nakagawa-Goto, P.C. Wu, S.L. Morris-Natschke, A. Brossi, K.F. Bastow, J.Y. Lang, M.C. Hung, K.H. Lee, Antitumor agents 270. Novel substituted 6-phenyl-4H-furo[3,2-c]pyran-4-one derivatives as potent and highly selective anti-breast cancer agents, Bioorg. Med. Chem. 18 (2010) 803–808.

[18] T. Song, X. Li, X. Chang, X. Liang, Y. Zhao, G. Wu, S. Xie, P. Su, Z. Wu, Y. Feng, Z. Zhang, 3-Thiomorpholin-8-oxo-8H-acenaphtho [1,2-b] pyrrole-9-carbonitrile (S1) derivatives as pan-Bcl-2-inhibitors of Bcl-2, Bcl-xL and Mcl-1, Bioorg. Med. Chem. 21 (2013) 11–20.
[19] Z. Zhang, G. Wu, F. Xie, T. Song, X. Chang, 3-Thiomorpholin-8-oxo-8H-acenaphtho[1,2-b]pyrrole-9-carbonitrile (S1) based molecules as potent, dual inhibitors of B-cell lymphoma 2 (Bcl-2) and myeloid cell leukemia sequence 1 (Mcl-1): structure-based design and structure-activity relationship studies, J. Med. Chem. 54 (2011) 1101–1105.
[20] E. Freire, Do enthalpy and entropy distinguish first in class from best in class, Drug Discovery Today 13 (2008) 869–874.
[21] G.G. Ferenczy, G.M. Keseru, Thermodynamics guided lead discovery and optimization, Drug Discovery Today 15 (2010) 919–932.
[22] G. Wang, Z. Nikolovska-Coleska, C.Y. Yang, R. Wang, G. Tang, J. Guo, S. Shangary, S. Qiu, W. Gao, D. Yang, J. Meagher, J. Stuckey, K. Krajewski, S. Jiang, P.P. Roller, H.O. Abaan, Y. Tomita, S. Wang, Structure-based design of potent small-molecule inhibitors of anti-apoptotic Bcl-2 proteins, J. Med. Chem. 49 (2006) 6139–6142.
[23] G. Hacker, A. Weber, BH3-only proteins trigger cytochrome c release, but how? Arch. Biochem. Biophys. 462 (2007) 150–155.
[24] H.M. Berman, J. Westbrook, Z. Feng, G. Gilliland, T.N. Bhat, H. Weissig, I.N. Shindyalov, P.E. Bourne, The protein data bank, Nucleic Acids Res. 28 (2000) 235–242.
[25] G.M. Morris, D.S. Goodsell, R.S. Halliday, R. Huey, W.E. Hart, R.K. Belew, A.J. Olson, Automated docking using a Lamarckian genetic algorithm and an empirical binding free energy function, J. Comput. Chem. 19 (1998) 1639–1662.